

Microporous and Mesoporous Materials

Thermal stability of templated ZSM-5 zeolites: an in-situ synchrotron X-ray powder diffraction study --Manuscript Draft--

Manuscript Number:	MICMAT-D-23-01075
Article Type:	Full length article
Keywords:	ZSM-5; TPA+; in situ synchrotron X-ray powder diffraction; thermal stability; structural evolution
Corresponding Author:	Enrico Catizzone University of Calabria ITALY
First Author:	Maura Mancinelli
Order of Authors:	Maura Mancinelli Nicola Precisvalle Matteo Ardit Giada Beltrami Lara Gigli Enrico Catizzone Massimo Migliori Girolamo Giordano Annalisa Martucci
Abstract:	<p>The topological symmetry of the as-synthesized ZSM-5 is orthorhombic Pnma, with 12 crystallographically independent tetrahedral sites in the unit cell. Its actual symmetry depends on the synthesis and post-synthesis treatment, SiO₂/Al₂O₃ ratio, structural defects, temperature, nature and amount of sorbate organic molecules. Highly crystallized ZSM-5 zeolite can be synthesized using organic species as structure directing agents (SDA), including tetra-n-propylammonium (TPA) and Na cations. The type and amount of organic and inorganic precursors in synthetic solutions influence the Al location in the MFI zeolite framework and consequently the material properties. The use of TPA as SDA has attracted increasing attention due to its intermediate hydrophobicity/hydrophilicity and its ability to tailor the physicochemical properties of ZSM-5, optimizing the selectivity of zeolite catalysts and the efficiency of the overall chemical process. This work investigates the thermal stability and high temperature structural evolution by in situ synchrotron powder diffraction of TPA-ZSM-5 with different Si/Al ratios (15, 25, 50, and 100) and their structural modifications induced by template calcination. Rietveld refinements of the room temperature data revealed that in all samples tetrapropylammonium ions are located at the intersection of the sinusoidal and the straight channels. The refined TPA⁺ content increases with the increasing of the Si/Al ratio of the zeolite, reaching the theoretical value of 4 when the Si/Al ratio =84, –in very good agreement with both chemical and thermogravimetric analyses. The bond distances evidenced the lack of interactions between the TPA⁺ and the framework oxygen atoms. The high temperature refinements confirmed the high thermal stability of all four ZSM-5 samples, which remain crystalline until the end of the thermal treatment (800 °C). Burning of the template does not cause any relevant variations in the framework geometry and channel shape, confirming the high flexibility of the MFI framework.</p> <p>In addition, thermal analysis proved insights about the effect of aluminum content on the interaction between SDA and zeolite structure.</p>

COVER LETTER

Prof. Heloise PASTORE

Editor-in-Chief

Microporous and Mesoporous Materials

Universidade Estadual de Campinas

Campinas, São Paulo, Brazil

Dear Prof. Pastore,

enclosed herewith you may find the copy of the following manuscript:

Thermal stability of templated ZSM-5 zeolites: an in-situ synchrotron X-ray powder diffraction study

by Maura Mancinelli, Nicola Precisvalle, Matteo Ardit, Giada Beltrami, Lara Gigli, Enrico Catizzone, Massimo Migliori, Girolamo Giordano and Annalisa Martucci

We would be grateful if you consider this original research paper for the publication in Microporous and Mesoporous Materials.

The paper deals with the investigation of the thermal behaviour of TPA⁺-templated ZSM-5 synthesised with different Si/Al ratio by means of synchrotron X-Ray diffraction technique. The study allows assessing the effect of aluminium content on the structural changes of ZSM-5 zeolite as a function of temperature and during the decomposition of TPA⁺ ions. At this regard, ZSM-5 were synthesised with a bulk Si/Al molar ratio equals to 21, 30, 50 and 84 and the synchrotron X-Ray patterns were acquired from room temperature to 800°C. The Rietveld refinements at room temperature indicate that the amount of TPA⁺ ions molecules per unit cell depends on the aluminium content and that the template ions are located at the intersection of the sinusoidal and the straight channels of MFI structure. The structural evolution as a function of temperature indicated that the thermal treatment does not affect the structure of the samples, also during the removal of the template, confirming the high thermal stability of ZSM-5 materials.

We hope that this contribution to the understanding of the thermal behaviour of templated ZSM-5 materials prepared with different chemical composition could be well hosted in your prestigious journal.

We also confirm that neither the manuscript nor its contents in any other form, has been previously published by any of the authors and/or is under consideration for publication in any other scientific journal.

On behalf of all the Authors

Yours sincerely

Prof. Annalisa Martucci



Dr. Enrico Catizzone



22 June, 2023

Prof. Annalisa Martucci

mrs@unife.it

University of Ferrara

Department of Physics and Earth Sciences

Via Saragat, 1

44100 – Ferrara, Italy

Tel: +39-(0)532-974730

Dr. Enrico CATIZZONE

enrico.catizzone@unical.it

University of Calabria

CECaSP_Lab

Via P. Bucci

87036 - Rende, Italy

Tel: +39 - 0984496651

Reviewer Suggestions

Prof. Heloise PASTORE

Editor-in-Chief
Microporous and Mesoporous Materials
Universidade Estadual de Campinas
Campinas, São Paulo, Brazil

Dear Prof. Pastore,

in relation to the following submitted manuscript

Thermal stability of templated ZSM-5 zeolites: an in-situ synchrotron X-ray powder diffraction study

by Maura Mancinelli, Nicola Precisvalle, Matteo Ardit, Giada Beltrami, Lara Gigli, Enrico Catizzone, Massimo Migliori, Girolamo Giordano and Annalisa Martucci

We indicate the following scientists and experts in the field of zeolite science and technology as potential reviewers:

- 1) Prof. Mirosław Derewinski, Member of Editorial Board of Microporous and Mesoporous Materials
derewinski@gmail.com.
- 2) Dr. Roberto Millini, ENI S.p.A., Italy, roberto.millini@eni.com
- 3) Prof. German Sastre, CSIC-UPV - Instituto de Tecnología Química (ITQ), Valencia, Spain, gsastre@itq.upv.es.
- 4) Prof. Suk Bong Hong, Pohang University of Science and Technology, Pohang, South Korea,
sbhong@postech.ac.kr.

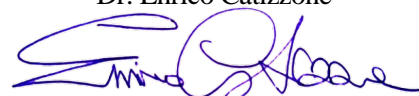
On behalf of all the Authors

Yours sincerely



Prof. Annalisa Martucci

Dr. Enrico Catizzone



22 June, 2023

Prof. Annalisa Martucci

mrs@unife.it

University of Ferrara

Department of Physics and Earth Sciences

Via Saragat, 1

44100 – Ferrara, Italy

Tel: +39-(0)532-974730

Dr. Enrico CATIZZONE

enrico.catizzone@unical.it

University of Calabria

CECaSP_Lab

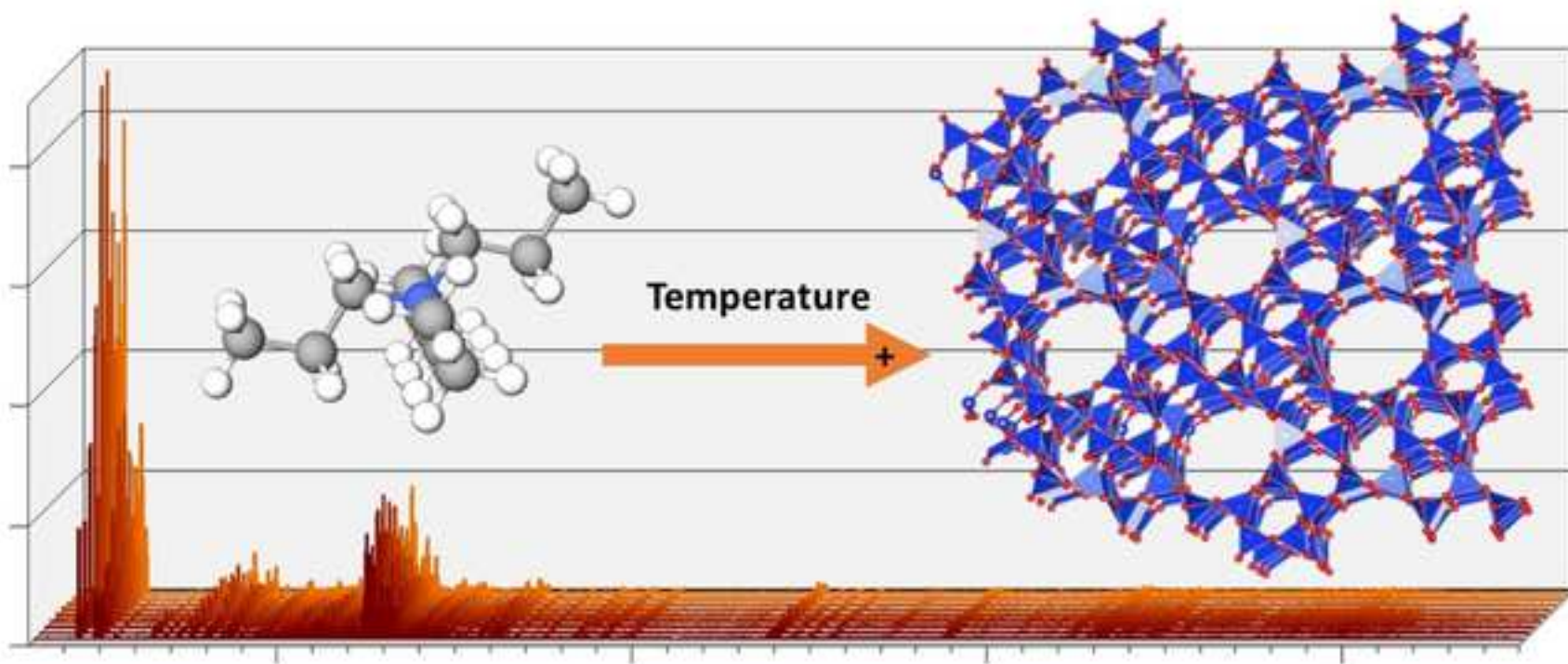
Via P. Bucci

87036 - Rende, Italy

Tel: +39 - 0984496651

HIGHLIGHTS

- The thermal stability of TPA⁺-ZSM-5 was assessed by synchrotron XRD.
- TPA⁺ is located at the channel's intersection regardless of the Si/Al ratio.
- ZSM-5 with higher Si/Al ratio hosts more TPA⁺ per unit cell.
- High thermal stability of ZSM-5 was confirmed up to 800°C.
- TPA⁺ removal does not affect framework geometry and channel shape of ZSM-5.



[Click here to view linked References](#)

1 **Thermal stability of templated ZSM-5 zeolites: an *in-situ*** 2 **synchrotron X-ray powder diffraction study**

3
4 Maura Mancinelli¹, Nicola Precisvalle¹, Matteo Ardit¹, Giada Beltrami¹, Lara Gigli², Enrico
5 Catizzone^{3*}, Massimo Migliori³, Girolamo Giordano³ and Annalisa Martucci^{1*}

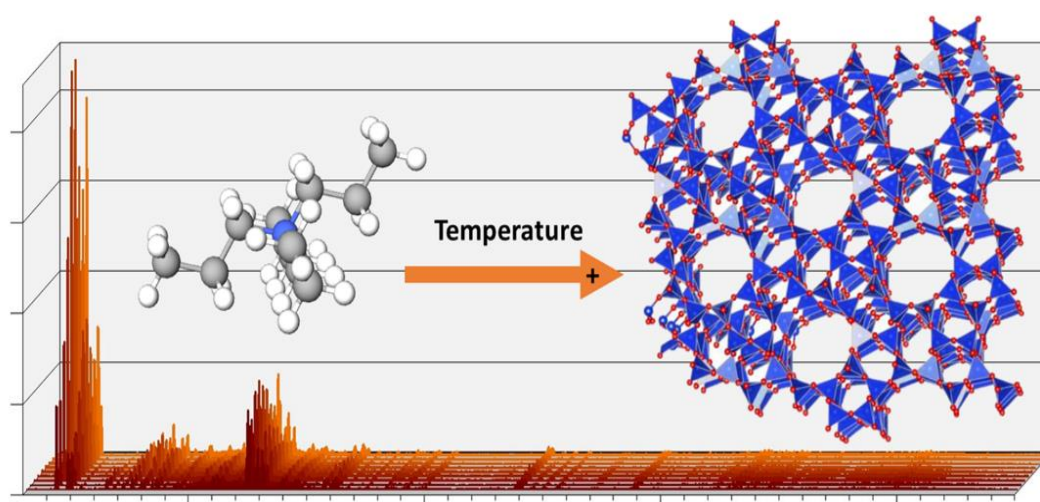
6
7 ¹ Department of Physics and Earth Sciences, University of Ferrara Via Saragat 1, I-44121, Ferrara,
8 Italy.

9 ² Elettra-Sincrotrone Trieste S.C.p.A., Beamline, Strada Statale 14 - km 163,5 in AREA Science Park,
10 Basovizza, Trieste, Italy.

11 ³ Chemical Engineering Catalysis and Sustainable Processes Laboratory, CECaSP_Lab - University of
12 Calabria, Via P. Bucci -87036 Rende (CS), Italy

13
14 Corresponding author e-mail: *enrico.catizzone@unical.it; *mrs@unife.it;

15 16 17 **Graphical Abstract**



18

19

1 **Abstract**

2 The topological symmetry of the as-synthesized ZSM-5 is orthorhombic *Pnma*, with 12
3 crystallographically independent tetrahedral sites in the unit cell. Its actual symmetry depends on the
4 synthesis and post-synthesis treatment, SiO₂/Al₂O₃ ratio, structural defects, temperature, nature and
5 amount of sorbate organic molecules. Highly crystallized ZSM-5 zeolite can be synthesized using
6 organic species as structure directing agents (SDA), including tetra-*n*-propylammonium (TPA) and Na
7 cations. The type and amount of organic and inorganic precursors in synthetic solutions influence the
8 Al location in the MFI zeolite framework and consequently the material properties. The use of TPA as
9 SDA has attracted increasing attention due to its intermediate hydrophobicity/hydrophilicity and its
10 ability to tailor the physicochemical properties of ZSM-5, optimizing the selectivity of zeolite catalysts
11 and the efficiency of the overall chemical process. This work investigates the thermal stability and
12 high temperature structural evolution by *in situ* synchrotron powder diffraction of TPA-ZSM-5 with
13 different Si/Al ratios (15, 25, 50, and 100) and their structural modifications induced by template
14 calcination. Rietveld refinements of the room temperature data revealed that in all samples
15 tetrapropylammonium ions are located at the intersection of the sinusoidal and the straight channels.
16 The refined TPA⁺ content increases with the increasing of the Si/Al ratio of the zeolite, reaching the
17 theoretical value of 4 when the Si/Al ratio =84, –in very good agreement with both chemical and
18 thermogravimetric analyses. The bond distances evidenced the lack of interactions between the TPA⁺
19 and the framework oxygen atoms. The high temperature refinements confirmed the high thermal
20 stability of all four ZSM-5 samples, which remain crystalline until the end of the thermal treatment
21 (800 °C). Burning of the template does not cause any relevant variations in the framework geometry
22 and channel shape, confirming the high flexibility of the MFI framework.
23 In addition, thermal analysis proved insights about the effect of aluminum content on the interaction
24 between SDA and zeolite structure.

25
26 **Keywords:** ZSM-5, TPA⁺, *in situ* synchrotron X-ray powder diffraction, thermal stability, structural
27 evolution.

1 Introduction

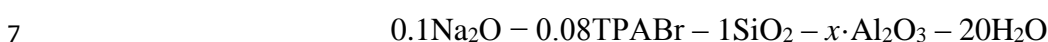
2 ZSM-5, the synthetic counterpart of the mutinaite mineral,
3 $[\text{Na}_{2.76}\text{K}_{0.11}\text{Mg}_{0.21}\text{Ca}_{3.78}][\text{Al}_{11.20}\text{Si}_{84.91}]\cdot 60\text{H}_2\text{O}$ [1], is characterized by a MFI framework topology and
4 a three-dimensional channels system. The structure is built on the intersection of two sets of tubular
5 channels, both defined by 10-membered ring openings: the straight channel (SC channel), parallel to
6 the [010] direction, and the sinusoidal channel (ZZ channel), parallel to the [100] direction. The free
7 diameters of the SC and ZZ channels are from 5.4 to 5.6 Å and 5.1 to 5.5 Å, respectively [2]. The
8 topological symmetry of the as-synthesized ZSM-5 (i.e., intended as ZSM-5 with
9 tetrapropylammonium template molecule inside the channel system) is the orthorhombic *Pnma*, with
10 12 crystallographically independent tetrahedral sites in the unit cell [3], but its actual symmetry
11 depends strongly on the synthesis and post-synthesis treatment, $\text{SiO}_2/\text{Al}_2\text{O}_3$ ratio, structural defects,
12 temperature, nature and amount of sorbate organic molecules [4,5]. Usually, highly crystallized ZSM-
13 5 zeolite can be synthesized using organic species as structure directing agents (SDA), including tetra-
14 *n*-propylammonium (TPA) and Na cations. The type and amount of organic and inorganic precursors
15 in synthetic solutions influence the Al location in the MFI zeolite framework and consequently the
16 material properties. The use of TPA as SDA has attracted increasing attention due to its intermediate
17 hydrophobicity/hydrophilicity and its ability to tailor the physicochemical properties (crystal size
18 and/or chemical composition) of ZSM-5, thus optimizing the selectivity of zeolite catalysts and the
19 efficiency of the overall chemical process [6]. In order to make the zeolite pores accessible to guest
20 molecules, the organic templates have to be removed by calcination in air from 25 to 550 °C [7]. The
21 template burning leaves behind one proton per each SDA complex for charge balancing, thus forming
22 Brønsted acid sites. The comprehension of the template thermally induced decomposition at the
23 molecular level is still a controversial issue and unambiguous interpretations have not yet been
24 achieved. The targets of this work are to investigate the thermal stability and high temperature
25 structural evolution of TPA-ZSM-5 with different Si/Al bulk ratios (21, 30, 51, and 84, respectively)

1 and to study their structural modifications induced by template calcination on the zeolite framework
2 by means of *in situ* synchrotron X-ray powder diffraction.

3

4 **Materials and Methods**

5 **Materials.** ZSM-5 zeolite samples (MFI topology, 3-dimensional channels system) were synthesized
6 at different Si/Al ratios starting from the following gel composition:



8 with the amount of Al_2O_3 varying in the range of $0.005 < x < 0.033$ mol, according to the expected
9 Si/Al molar ratio in the gel, namely: 15, 25, 50 and 100 mol/mol. The synthesis gel was prepared by
10 adding 2.66 g of sodium hydroxide (97%, Carlo Erba Reagenti) to 119.40 mL of distilled water [8–
11 10]. Aluminum hydroxide (98%, Fluka) was dissolved in the basic solution with 7.10 g of
12 tetrapropylammonium bromide (98%, Fluka), and the resulting solution was added to the gel. The
13 addition of 19.95 g of precipitated silica (100%, Merck) was followed by stirring for 2 h at room
14 temperature (*RT*). Crystallization was carried out at 175 °C in a PTFE-lined stainless steel static
15 autoclave (0.150 L). After 96 h of crystallization, the solid phase was filtered, washed with distilled
16 water and dried at 100 °C overnight. The bulk Si/Al molar ratio was determined by both atomic
17 absorption spectroscopy using a GBC 932 instrument [11] and Energy-dispersive X-ray spectroscopy
18 (Phenom ProX) and data are summarized in Table 1. TG/DTA data of as-synthesized samples were
19 acquired (TA Instruments SDT 650) up to 850 °C (heating rate: 5 °C/min) under 100 mL/min of air
20 flow. After calcination (air flow, 500°C for 4 h), SEM-EDX of Na-form of the samples, where also
21 acquired (Phenom Pro G6, Thermo Fisher)[12].

22 Even though the presence of extra-framework Al cannot be excluded (especially for samples with low
23 Si/Al ratio), data shows an increasing of TPA^+ incorporation as counterion when increasing the Si/Al
24 ratio of the zeolite, reaching the theoretical value of 4 when the Si/Al ratio is equal to 84.

25

26

1 **Table 1.** Si/Al ratio of templated ZSM-5 samples in gel and in bulk.
2

Sample	Gel Si/Al ratio [mol/mol]	Bulk Si/Al ratio AAS [mol/mol]	Bulk Si/Al ratio EDX [mol/mol]
ZSM-5t_21	15	21	11
ZSM-5t_30	25	30	13
ZSM-5t_51	50	51	20
ZSM-5t_84	100	84	43

3
4 **TDA-TGA analysis.** The charts are reported in Fig SI.3 of Supplementary information and the TGA
5 elaboration allows to calculate the TPA⁺ weight loss for all the samples and the TPA⁺ per unit cell,
6 assuming the full incorporation of the Aluminum within the framework (Table 2).
7

8 **Table 2.** TPA⁺ weight loss and theoretical calculation per unit cell
9

Sample	Al ³⁺ per u.c. [mol]	TPA ⁺ per u.c [mol]	TPA ⁺ under LT peak [%w/w]	TPA ⁺ under HT peak [%w/w]	LT/(LT+HT) [-]
ZSM-5t_21	4.36	3.3	3.2%	8.2%	0.28
ZSM-5t_30	3.10	3.5	3.7%	7.6%	0.33
ZSM-5t_51	1.85	3.7	5.2%	7.2%	0.42
ZSM-5t_84	1.13	4.0	6.0%	7.0%	0.46

10
11 A common feature of all the samples was found in a double peak in DTA analysis: a low-one (LT with
12 the peak in the range: 414°C - 420°C) related to the weak interaction of TPA⁺ with a part of AlO₄⁻ (and
13 silanol groups) and a high-one (LT with the peak in the range: 471°C – 493°C) attributed to the strong
14 interaction with the rest of AlO₄⁻. The deconvolution of the TGA derivative vs time allowed to attribute
15 the relative amount of TPA⁺ interacting with the zeolite structure in a weak and strong manner,
16 respectively, and data reported in the last three columns of Table 2. Results indicate that fraction of
17 weakly interacting TPA⁺ increases as the aluminum content decreases. The higher fraction of strongly
18 bonded TPA⁺ can be associated to the TPA⁺ interacting with AlO₄⁻ framework species, according to
19 the Al content increase in the samples.

1 SEM micrographs of the investigated samples are reported in Figure SI4. All the samples exhibit
2 prismatic larger crystals approximately 6-10 μm in size accompanied by smaller crystals
3 approximately 1-2 μm .

4
5 **Synchrotron X-ray Powder Diffraction.** X-ray powder patterns as a function of temperature were
6 collected at the MCX beamline [13,14] of the Elettra synchrotron light source (Trieste, Italy) in
7 transmission geometry on a 4-circle Huber diffractometer equipped with a fast scintillator detector
8 with a high-count rate, preceded by a pair of slits with a vertical aperture of 200 and 300 μm ,
9 respectively. Each sample was loaded into an axially spinning quartz capillary ($\varnothing=0.5$ mm) previously
10 mounted on a goniometric head. The sample temperature was varied and monitored using a gas blower.
11 The experimental conditions for each temperature studied were $\lambda=0.82700(1)$ \AA (15 KeV), 2θ angular
12 range = 3–45°, step size = 0.005° 2θ , counting time per step = 1 s. X-ray powder diffraction patterns
13 were recorded every 100 °C from *RT* to 800 °C in air at a heating rate of 5 °C min^{-1} .

14
15 **Refinement Strategy.** Full-profile Rietveld refinements were performed using the GSAS software
16 and the EXPGUI graphical interface [15,16]. The crystal structure of ZSM-5 collected at *RT* was
17 refined starting from the structure model of the topological ZSM-5 (orthorhombic, s.g. *Pnma*) by Van
18 Koningsveld et al. [3]. Peak profile modeling was performed using a pseudo-Voigt function with the
19 peak cut-off set to 0.05% of the peak intensity maximum, two Gaussian terms (θ -independent *GW*,
20 $\tan\theta$ dependent *GV*, respectively) and two Lorentzian broadening coefficients ($\cos\theta^{-1}$ - and $\tan\theta$ -
21 dependent, *LX* and *LY*, respectively) plus an asymmetry contribution (*asym*) and two terms to
22 reproduce the anisotropic contributions of the Lorentzian broadening (*ptec* and *stec*). In addition to 26
23 shifted Chebyshev polynomial coefficients to fit the background and a shift contribution (*shift*) to
24 account for the sample displacement, the refinements included unit-cell parameters, atomic
25 coordinates, and atomic displacement parameters (ADPs, U_{iso}). During the refinement of the

1 framework atomic coordinates, a set of soft constraints were applied to the tetrahedral T–O and O–O
 2 bond distances (1.60 and 2.60 Å, respectively, with $\sigma = 0.04$ Å). The restraint weight (F) was
 3 progressively reduced in the final refinement cycles until the atomic coordinates were allowed to vary
 4 almost freely (*i.e.*, the calculated standard deviation of the bond lengths was smaller than the tolerance
 5 applied to the constrained bond distances). ADPs were constrained in order to have the same value for
 6 the same atomic species. The atomic coordinates of the tetrapropylammonium organic structure
 7 directing agent (TPA⁺) were derived from residuals of the electron density calculated from the
 8 difference Fourier maps. No residuals for H and Na atoms were detected due to both the low H atomic
 9 scattering factor and the high atomic disorder of H and Na within the zeolite lattice. The extra-
 10 framework atomic coordinates were refined by imposing soft constraints on the N–C (*i.e.*, 1.48 and
 11 2.48 Å, $\sigma = 0.04$ Å) and C–C (*i.e.*, 1.42 and 2.70 Å, $\sigma = 0.04$ Å) bond distances to preserve the TPA⁺
 12 molecular geometry. In addition, the atomic fraction and ADPs for the N and C atoms of the TPA⁺
 13 molecule were constrained to vary equally.

14 Details of the data collection and refinement agreement factors are given in Table 3.

16 **Table 3.** Details of XRPD data collection at *RT* and refinement agreement indices.

TPA ⁺ -ZSM-5 (s.g. <i>Pnma</i> , Z = 8)				
λ (Å) = 0.82700(1)				
Refined 2θ (°) range = 3–45				
No. of data = 8400				
No. of variable = 156				
	ZSM-5t_21	ZSM-5t_30	ZSM-5t_51	ZSM-5t_84
R_{wp}	0.216	0.156	0.140	0.188
R_p	0.161	0.119	0.104	0.140
R_{F^2}	0.102	0.128	0.124	0.102

18
 19 Framework atomic coordinates, site atomic fractions, and ADPs for samples at *RT* are reported as
 20 Supplemental Information (SI) in Tables SI1 to SI4. The atomic coordinates, site atomic fractions, and

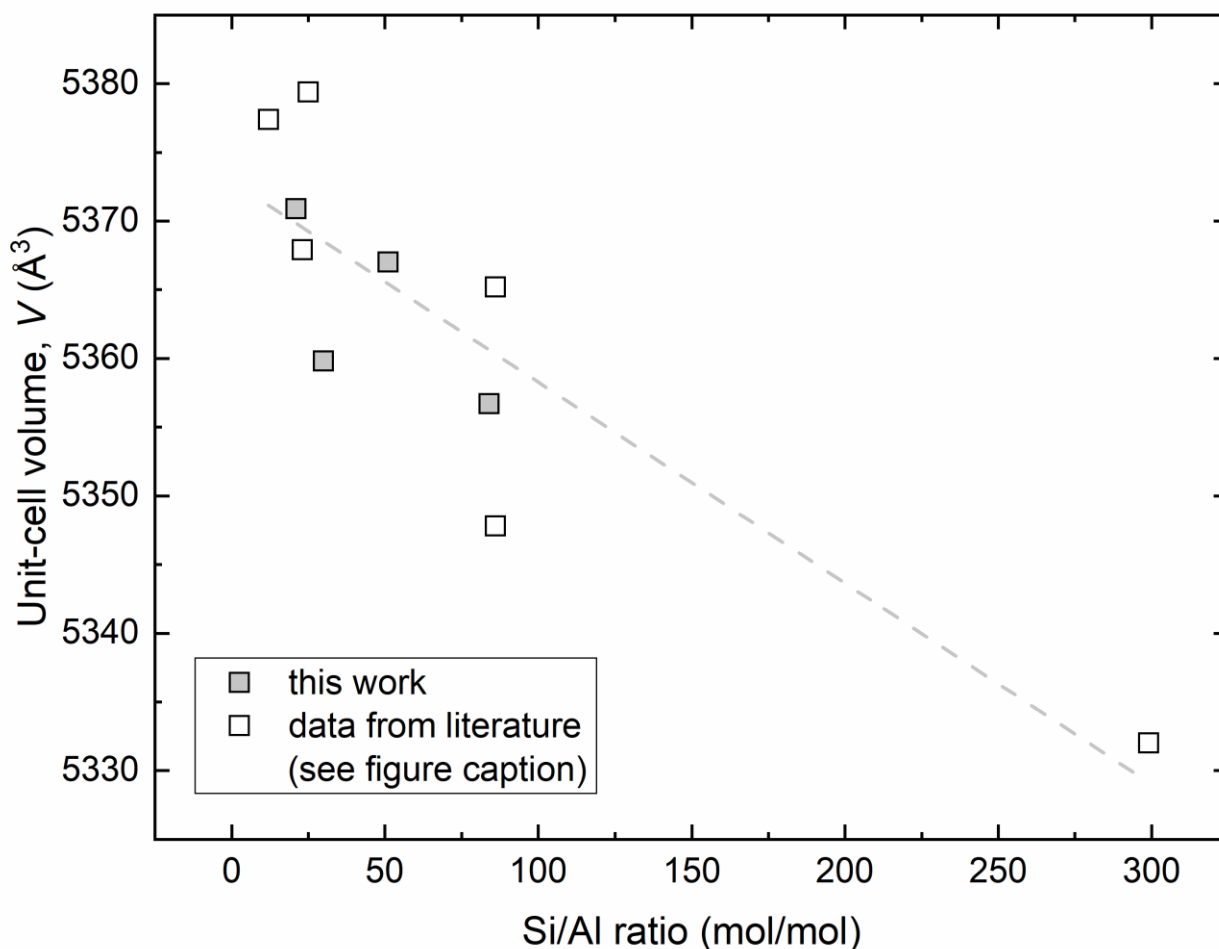
ADPs for the TPA⁺ extra-framework molecule at *RT* are reported in Table SI5. In addition, Tables SI6 to SI21 list framework atomic coordinates, site atomic fractions, and ADPs for all investigated samples at selected temperatures (*i.e.*, 200, 400, 600, and 800 °C).

Results and Discussion

Structural Refinements at *RT*. The crystal structure of ZSM-5 synthesized using TPA⁺ molecules as templating agent, has been previously investigated by several authors [3,17–21]. All of these zeolites, as well as those investigated in this work, are characterized by the ZSM-5 topological structure, which crystallizes in the orthorhombic crystal system (s.g. *Pnma*) with 12 independent tetrahedral sites in the unit cell. A comparison between the investigated samples and those from the literature shows that the lattice parameters vary significantly with the aluminum content (*i.e.*, Si/Al ratio), with a volumetric variation ranging from 5332 Å³ to 5379 Å³ for samples with Si/Al ratios of 299 and 25 mol/mol, respectively (see Table 4). The tendency of a volumetric shrinkage as a function of Al content shown in Figure 1 is expected from stoichiometric considerations. Indeed, the ionic radius of Al³⁺ at the tetrahedral site is 50% larger than that of Si⁴⁺ in the same coordination (*i.e.*, 0.39 Å vs. 0.26 Å, respectively [22]).

Table 4. Unit-cell parameters of ZSM-5 zeolites at *RT* synthesized via *n*TPA⁺ templating molecule (0<*n*<4 molecules per unit cell pore-fillings).

TPA ⁺ -ZSM-5 (s.g. <i>Pnma</i> , Z = 8)										
	ZSM-5t_21	ZSM-5t_30	ZSM-5t_51	ZSM-5t_84	Ref.	Ref.	Ref.	Ref.	Ref.	Ref.
					[17]	[15]	[16]	[14]	[18]	[3]
<i>a</i> (Å)	20.048(4)	20.044(4)	20.062(3)	20.049(1)	20.092	20.072	20.100	20.07	20.044	20.022
<i>b</i> (Å)	19.966(4)	19.939(4)	19.945(3)	19.933(1)	19.952	19.937	19.959	19.92	19.918	19.899
<i>c</i> (Å)	13.418(2)	13.411(3)	13.413(2)	13.404(1)	13.414	13.414	13.409	13.42	13.395	13.383
<i>V</i> (Å ³)	5370.9(2)	5359.8(2)	5367.0(4)	5356.7(7)	5377.4	5367.9	5379.4	5365.2	5347.8	5332.0
Si/Al	21	30	51	84	12	23	25	86	86	299



2

3

4

5

6

7

8

9

10

11

12

Figure 1. Unit cell volume as a function of Si/Al ratio. Unit-cell volume and Si/Al ratio refer to data reported in Table 3. Dashed lines are a reader's guide. Symbol sizes exceed the estimated measurements uncertainties.

As far as the crystal structure at *RT* of the investigated ZSM-5 samples is concerned, subtle variations are observed with *T*–O bond distances and O–*T*–O bond angles ranging from 1.586(5) Å to 1.598(1) Å and from 108° to 110°, respectively (Tables SI22–SI25). On the contrary, the intertetrahedral *T*–O–*T* bond angles are characterized by a higher variability, suggesting that both the aluminum content and presence of TPA⁺ molecules influence the geometry of the zeolite channels even at *RT*, exerting a kind of chemical pressure [23,24]. Indeed, the *T*–O–*T* bond angles range from 140 to 173°, with equivalent angles for the compared samples differing by less than 10° (Tables SI22–SI25).

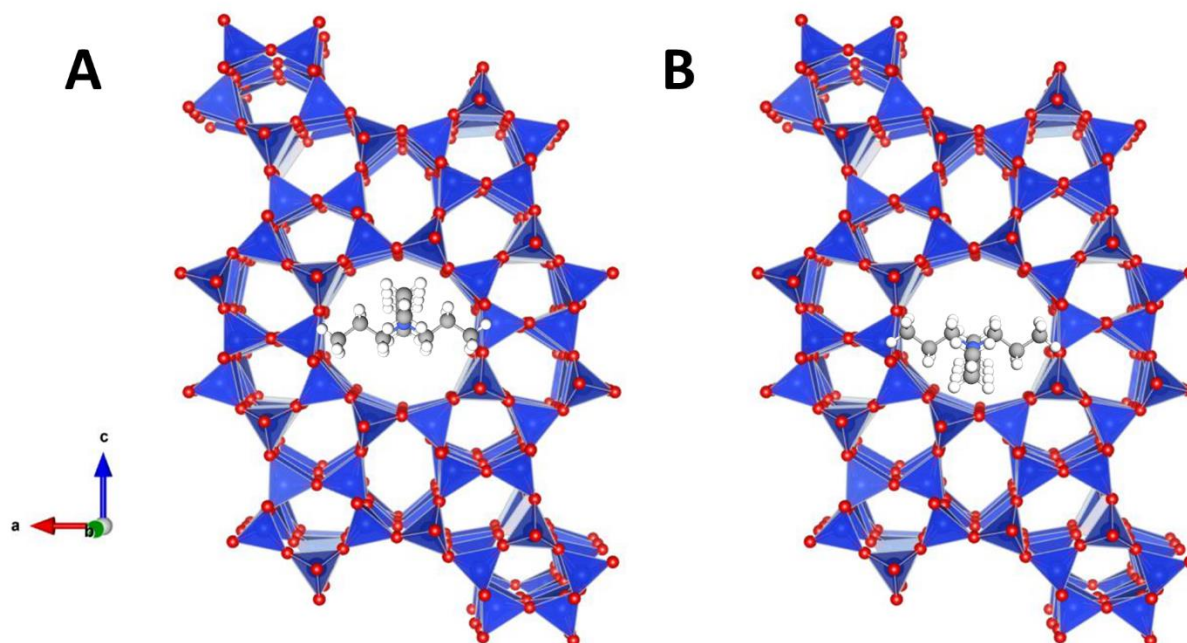
1 The channel distortions in zeolite systems are usually quantified as the departure from an ideal channel
 2 with a circular cross section, i.e., by calculating the ellipticity parameter ε , which is defined as the ratio
 3 between the longest and the shortest O–O bond distances that define the minimum and the maximum
 4 channel diameters, respectively. The data shown in Table 5 indicate that the straight (SC) and
 5 sinusoidal entrance (ZZ-A) channels are quite distorted ($\varepsilon = 1.09$ on average), while the sinusoidal exit
 6 (ZZ-B) is more regular ($\varepsilon = 1.04$ on average). These values, as well as other structural parameters,
 7 seem to be little or unaffected by the aluminum content. The crystallographic free area (CFA) sensu
 8 Baerlocher (*i.e.*, calculates as $\pi \times (\text{channel mean radius})^2$ in \AA^2 [25], shows that the channel apertures
 9 have a different CFA. On average, $\text{CFA}(\text{ZZ-A}) = 22.9 \text{ \AA}^2$, $\text{CFA}(\text{SC}) = 23.6 \text{ \AA}^2$, $\text{CFA}(\text{ZZ-B}) = 24.1$
 10 \AA^2 , with sinusoidal channels characterized by the smallest (ZZ-A) and the largest (ZZ-B) CFA,
 11 respectively.

12
 13 **Table 5.** Ellipticity (ε) and crystallographic free area (CFA) parameters for the investigated zeolite
 14 samples at *RT*.

	Channel	ZSM-5t_21	ZSM-5t_30	ZSM-5t_51	ZSM-5t_84
ε	SC	1.082	1.104	1.084	1.080
	ZZ-A	1.086	1.085	1.078	1.083
	ZZ-B	1.037	1.045	1.050	1.040
CFA (\AA^2)	SC	23.56	23.61	23.65	23.60
	ZZ-A	22.95	22.90	22.84	22.79
	ZZ-B	24.30	24.22	24.03	24.02

15
 16 According to Van Koningsveld et al. [3], residuals of electron density calculated using difference
 17 Fourier maps suggest that the TPA^+ molecule is located at the intersection of the sinusoidal and straight
 18 channels. Due to the presence of a mirror plane m at the center of the TPA^+ molecule, the molecule
 19 can statistically adopt two different crystallographic orientations depending on the distribution of the
 20 four propyl groups around the central nitrogen (Figure 2).

1 Rietveld refinements of the atomic occupancy indicate that the as-synthesized ZSM-5 sample with the
2 Si/Al ratio is equal to 84 contains four molecules per unit cell of TPA⁺ molecules, *i.e.*, the maximum
3 theoretical number of TPA⁺ molecules within the channels for a ZSM-5 zeolite [26].

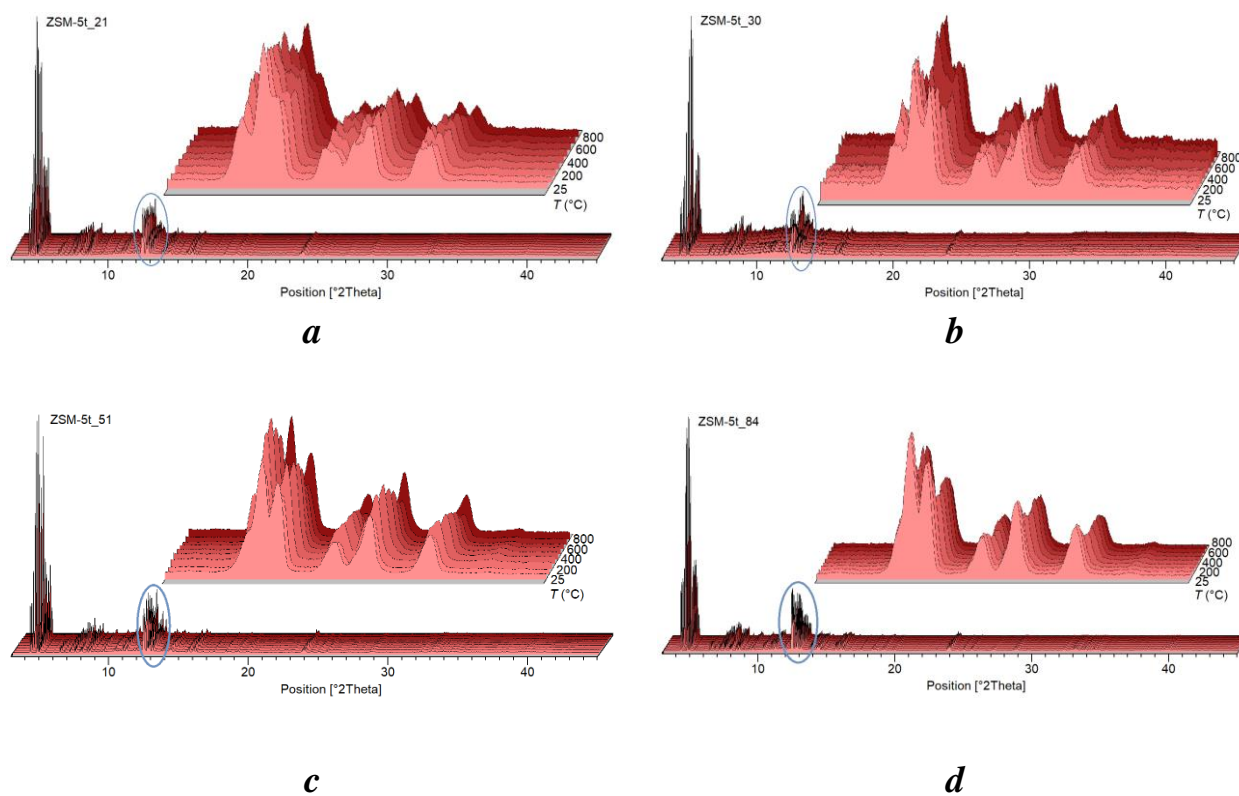


4 **Figure 2.** Polyhedral representation of the ZSM-5 structure along the [010] direction. TPA⁺ is located at the
5 intersection of the straight and sinusoidal channels. A and B refer to the possible orientations of TPA⁺.
6

7
8 In the other samples, the refined TPA⁺ content decreases with the lowering of the Si/Al ratio of the
9 zeolite (~3.3, 3.5 and 3.7 molecules per unit cell in ZSM-5 with Si/Al equal to 51, 30 and 21,
10 respectively), –in very good agreement with both chemical (Table 1) and thermogravimetric analyses
11 (Table 2). Since no additional electron density residuals were detected from the Fourier map
12 calculation, it can be argued that no co-adsorbed water molecules are present within the zeolite lattice.

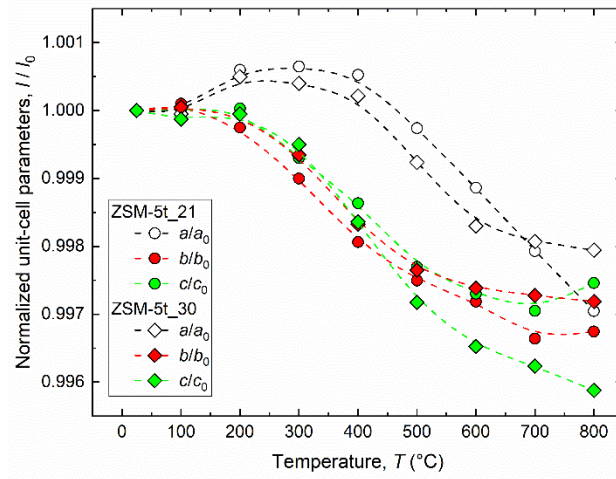
13
14 **High Temperature (HT) Structural Refinements.** Information on the kinetics of TPA⁺
15 decomposition, as well as structural variations due to the release of extra-framework components and
16 the resulting framework rearrangement, can be determined from *in-situ* X-ray diffraction data collected

1 at *HT*. The cascade plots in Figure 3 show the evolution of the investigated as-synthesized ZSM-5
2 samples in the temperature range *RT*–800 °C.

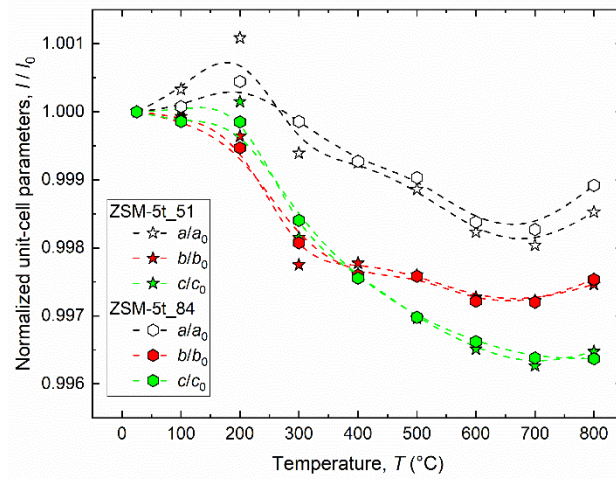


3 **Figure 3.** Cascade plots of ZSM-5t_21, ZSM-5t_30, ZSM-5t_51, and ZSM-5t_84 zeolites (from *a* to *d*,
4 respectively), and pattern details in the 4–5° and 10–15° 2θ angular ranges, within insets.

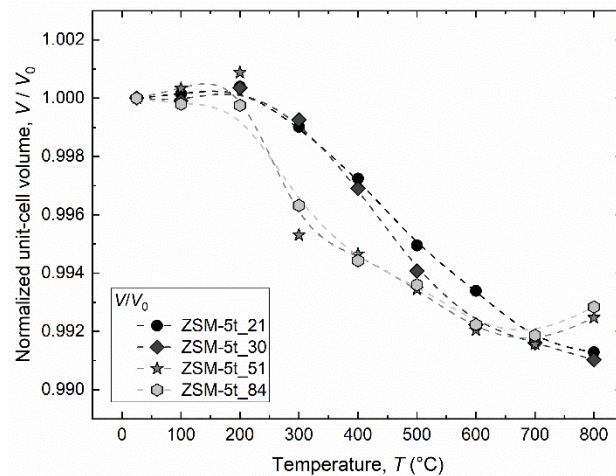
5
6 No evidence of crystallinity loss (peak broadening or collapse) is observed up to 800 °C, demonstrating
7 the high thermal stability of all as-synthesized ZSM-5 samples. Temperature-induced variations in
8 both peak positions and intensities are observed for all samples investigated. In particular, up to about
9 300 °C, peaks shift to lower 2θ angles, while at higher temperatures a peak shift to higher 2θ angles is
10 observed. This means that an initial lattice expansion (up to 300 °C) is followed by a unit-cell reduction
11 up to the maximum investigated temperature. A lattice contraction can be related to the progressive
12 removal of organic molecules during a thermal decomposition process[27–30]. Further clues to this
13 process can be derived from the peak intensity variations (mainly related to changes in structural
14 parameters) upon heating, as will be discussed later. The variation of the lattice parameters and the
15 unit-cell volume as a function of temperature (normalized to their value at *RT*) is shown in Figure 4.



a



b



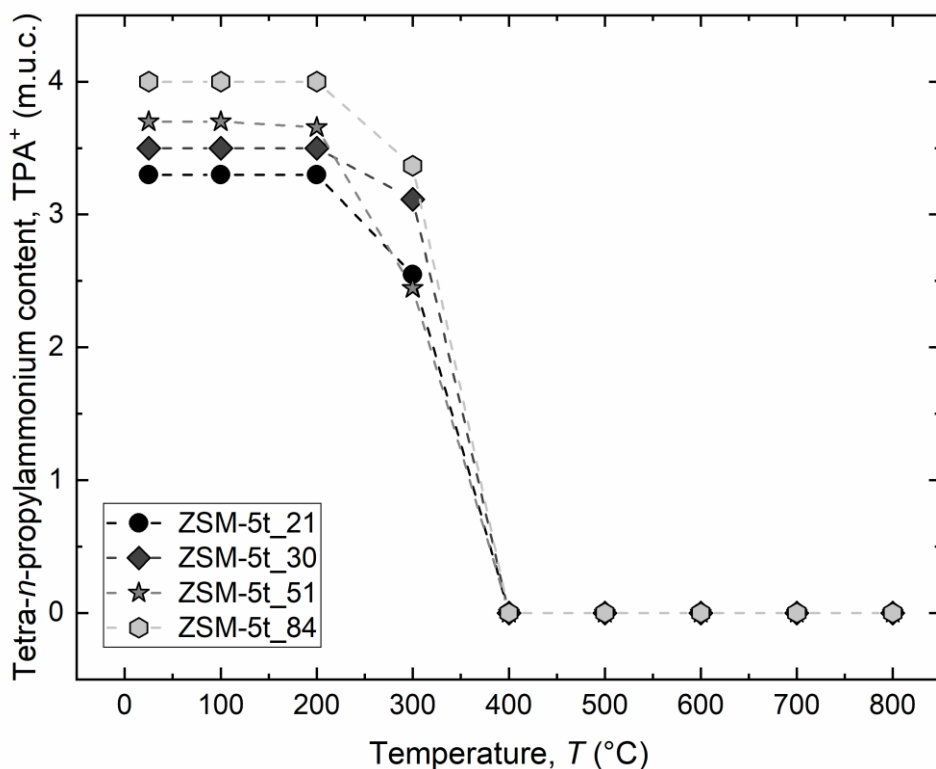
c

1

2 **Figure 4.** Lattice parameters evolution with temperature for samples ZSM-5t_21, and ZSM-5t_30 (*a*) and ZSM-
 3 5t_51 and ZSM-5t_84 (*b*), and temperature-dependence of unit-cell volume for all as-synthesized ZSM-5
 4 samples (*c*).

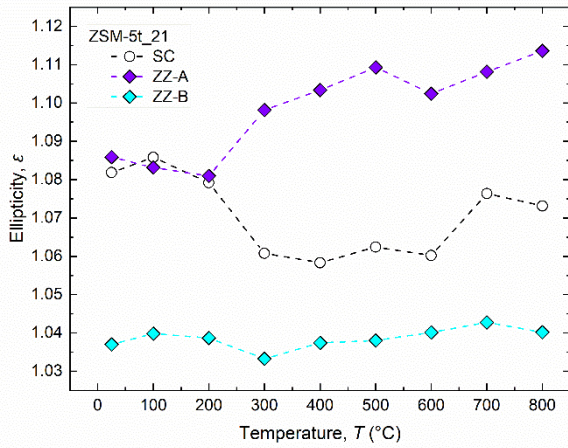
1 Based on their thermal evolution and according to the aluminum content, two different trends can be
2 rationalized for the pair of samples ZSM-5t_21 - ZSM-5t_30, and ZSM-5t_51 - ZSM-5t_84. In
3 agreement with Sen et al. [31], the concentration of Al³⁺ ions seems to be a discriminating factor during
4 the thermal evolution of orthorhombic H-ZSM-5 zeolites. Although at different rates, all investigated
5 zeolite samples are initially affected (to a lesser extent for the sample ZSM-5t_84) by a temperature-
6 induced positive thermal expansion up to 200 °C. At higher temperatures, the pairs of samples ZSM-
7 5t_21 - ZSM-5t_30, and ZSM-5t_51 - ZSM-5t_84 behave differently, with samples ZSM-5t_21 and
8 ZSM-5t_30 (those characterized by the highest aluminum content) undergoing a regular volumetric
9 contraction up to 800 °C. Differently, samples ZSM-5t_51 and ZSM-5t_84 show a steep volumetric
10 drop up to 300 °C, followed by a more gradual volumetric contraction up to 700 °C. In agreement with
11 Sen et al. [31], all samples show a negative thermal expansion in the 200-700 °C temperature range.
12 At the highest temperatures studied (*i.e.*, from 700 to 800 °C), samples ZSM-5t_51 and ZSM-5t_84
13 are characterized by a volumetric expansion. The total volume reduction over the investigated thermal
14 range is 0.87% and 0.89% for samples ZSM-5t_21 and ZSM-5t_30, and 0.75% and 0.71% for samples
15 ZSM-5t_51 and ZSM-5t_84, *i.e.*, the lower the Al³⁺ content, the lower the cell volume reduction. This
16 trend is consistent with that observed for a high-silica orthorhombic polymorph of H-ZSM-5 (Si/Al =
17 140) and for a silicalite-1 sample [32,33], where a volume reduction of 0.52% was found in the same
18 temperature range. Figure 5 shows the variation of the TPA⁺ content as a function of temperature.
19 Refinement of the site atomic fractions (site occupancies) shows that the crystallographic sites hosting
20 the templating molecule are unchanged up to 200 °C. At higher temperatures, the decomposition and
21 release process of TPA⁺ takes place for all the samples studied and, although with some small
22 differences, it is completed at 400 °C when all the crystallographic sites are completely empty. The
23 degradation of the TPA⁺ between 200 °C and 400 °C could explain the enhanced volumetric reduction
24 observed for the samples with the lowest aluminum content (*i.e.*, ZSM-5t_51 and ZSM-5t_84) in this
25 temperature range. The three-dimensional arrangement of tetrahedra sharing corners in ZSM-5 zeolite

1 structures confers a high framework flexibility. In fact, all the investigated samples, although subjected
 2 to a high thermal regime, show slight variations in both $T-O$ bond distances and $T-O-T$ bond angles,
 3 indicating that their framework does not undergo to relevant structural distortions.

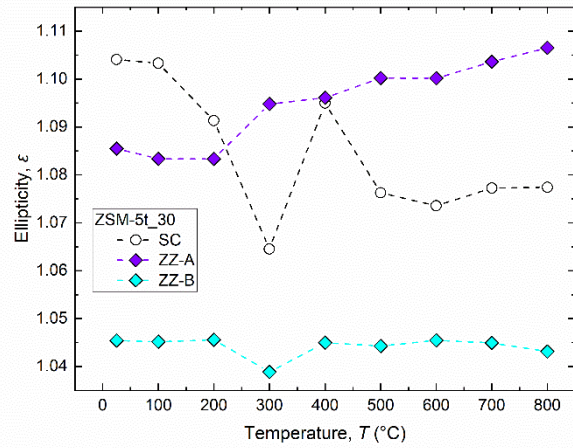


4 **Figure 5.** Content of extra-framework TPA⁺ molecules as a function of temperature.
 5
 6

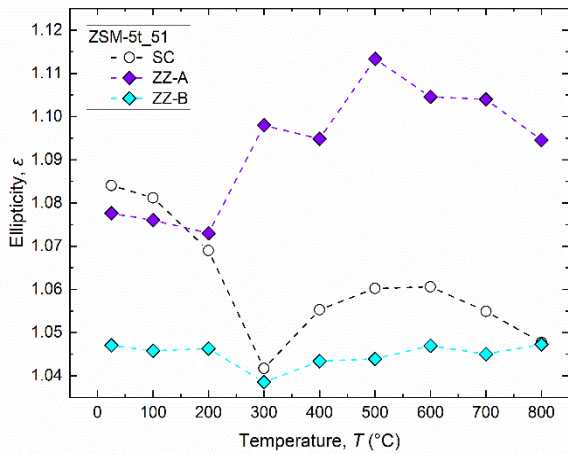
7 The $T-O$ bond distances and $T-O-T$ bond angles for selected temperatures (*i.e.*, 200, 400, 600, and
 8 800 °C) are listed in Tables SI22-SI25. This is also evidenced by the temperature variation of the
 9 ellipticity parameter for zeolite channels. While the ellipticity of ZZ-B channels is almost constant for
 10 all the samples over the whole temperature range (*i.e.*, ε fluctuates around 1.4), the heating process
 11 induces a variation in the shape of both ZZ-A and SC channels (Figure 6). In particular, two opposite
 12 trends can be observed: an increase in the ellipticity of the ZZ-A channel (evidence of a progressive
 13 departure from the circular shape) is associated with a decrease in the ellipticity (regularization) of the
 14 SC channel. Although some inhomogeneous variations can be observed for samples 423 and 422 due
 15 to the depletion of TPA⁺ at the earlier heating stages (*i.e.*, between 200 and 300 °C), the 10MR channel
 16 of all the samples studied tends to become more regular, although never reaching a circular shape.



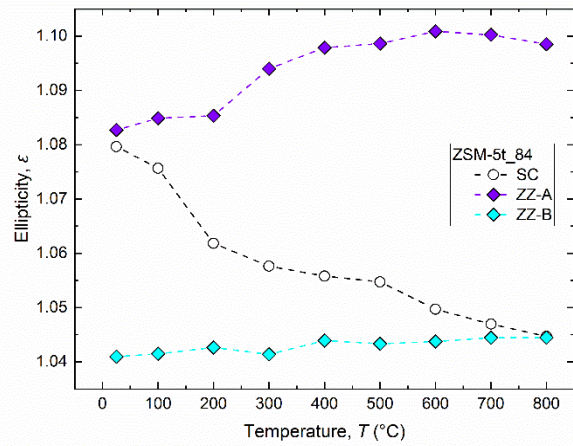
a



b



c



d

1 **Figure 6.** Ellipticity evolution of samples ZSM-5t_21, ZSM-5t_30, ZSM-5t_51 and ZSM-5t_84 (*a* to *d*) at *HT*.

2

3 The thermal treatment also induced slight changes in the CFA of the as-synthesized ZSM-5 zeolites
 4 (Figures SI2-SI5). Evidence of pore diameter reduction upon heating can be inferred from the decrease
 5 in CFA values for both SC and ZZ-A channels. In contrast, the effect of the heating process is less
 6 pronounced in the ZZ-B channel.

7

8 CONCLUSIONS

9 *In situ* synchrotron powder diffraction allowed monitoring the progressive thermal activation of four
 10 TPA⁺ templated ZSM-5 characterized by different Si/Al ratios. Rietveld refinements of the room

1 temperature data highlighted that in all the samples tetrapropylammonium ions are located at the
2 intersection of the sinusoidal and the straight channels. The refined TPA⁺ content increases with the
3 increasing of the zeolite Si/Al ratio, reaching the theoretical value of 4 when the Si/Al ratio =84, –in
4 very good agreement with both chemical and thermogravimetric analyses. The analysis of the bond
5 distances evidenced the lack of interactions between the TPA⁺ and the framework oxygen atoms.
6 Furthermore, the ellipticity parameters showed that the geometry of the channels is slightly distorted
7 since the beginning of the thermal treatment. The high temperature refinements confirmed the high
8 thermal stability of all four ZSM-5 samples, which remain crystalline until the end of the thermal
9 treatment (800 °C). The complete activation of ZSM-5 occurs between 300 and 400 °C, when the
10 TPA⁺ template is completely removed from the pores. Burning of the template does not cause any
11 relevant variations in the framework geometry and channel shape, confirming the high flexibility of
12 the MFI framework.

13

14 **Acknowledgments**

15 Project funded under the National Recovery and Resilience Plan (NRRP), Mission 04 Component 2
16 Investment 1.5 – NextGenerationEU, Call for tender n. 3277 dated 30/12/2021, Award Number:
17 0001052 dated 23/06/2022.

18

19 **References**

20

- 21 [1] G. Vezzalini, S. Quartieri, E. Galli, A. Alberti, G. Cruciani, Å. Kvik, Crystal structure of the
22 zeolite mutinaite, the natural analog of ZSM-5, *Zeolites*. 19 (1997) 323–325.
23 [https://doi.org/10.1016/S0144-2449\(97\)00124-3](https://doi.org/10.1016/S0144-2449(97)00124-3).

- 1 [2] H. Van Koningsveld, J.C. Jansen, A.J.M. De Man, Single-crystal structure analysis and energy
2 minimizations of a MFI-type zeolite at low p-dichlorobenzene sorbate loading, *Urn:Issn:0108-*
3 *7681. 52 (1996) 131–139.* <https://doi.org/10.1107/S0108768195008512>.
- 4 [3] H. Van Koningsveld, H. Van Bekkum, J.C. Jansen, On the location and disorder of the
5 tetrapropylammonium (TPA) ion in zeolite ZSM-5 with improved framework accuracy,
6 *Urn:Issn:0108-7681. 43 (1987) 127–132.* <https://doi.org/10.1107/S0108768187098173>.
- 7 [4] H. van Koningsveld, F. Tuinstra, J.C. Jansen, H. van Bekkum, On the preparation of a
8 monoclinic (nearly) single crystal of zeolite HZSM-5, *Zeolites. 9 (1989) 253–256.*
9 [https://doi.org/10.1016/0144-2449\(89\)90035-3](https://doi.org/10.1016/0144-2449(89)90035-3).
- 10 [5] H. van Koningsveld, J.C. Jansen, H. van Bekkum, The monoclinic framework structure of
11 zeolite H-ZSM-5. Comparison with the orthorhombic framework of as-synthesized ZSM-5,
12 *Zeolites. 10 (1990) 235–242.* [https://doi.org/10.1016/0144-2449\(94\)90134-1](https://doi.org/10.1016/0144-2449(94)90134-1).
- 13 [6] M. Moliner, F. Rey, A. Corma, Towards the Rational Design of Efficient Organic Structure-
14 Directing Agents for Zeolite Synthesis, *Angewandte Chemie International Edition. 52 (2013)*
15 *13880–13889.* <https://doi.org/10.1002/ANIE.201304713>.
- 16 [7] I. Jirka, P. Sazama, A. Zikánová, P. Hrabánek, M. Kocirik, Low-temperature thermal removal
17 of template from high silica ZSM-5. Catalytic effect of zeolitic framework, *Microporous and*
18 *Mesoporous Materials. 137 (2011) 8–17.*
19 <https://doi.org/10.1016/J.MICROMESO.2010.08.015>.
- 20 [8] M. Migliori, A. Aloise, E. Catizzone, G. Giordano, Kinetic analysis of methanol to dimethyl
21 ether reaction over H-MFI catalyst, *Ind Eng Chem Res. 53 (2014) 14885–14891.*
22 https://doi.org/10.1021/IE502775U/SUPPL_FILE/IE502775U_SI_001.PDF.

- 1 [9] A. Aloise, A. Marino, F. Dalena, G. Giorgianni, M. Migliori, L. Frusteri, C. Cannilla, G.
2 Bonura, F. Frusteri, G. Giordano, Desilicated ZSM-5 zeolite: Catalytic performances
3 assessment in methanol to DME dehydration, *Microporous and Mesoporous Materials*. 302
4 (2020) 110198. <https://doi.org/10.1016/J.MICROMESO.2020.110198>.
- 5 [10] G. Bonura, C. Cannilla, L. Frusteri, E. Catizzone, S. Todaro, M. Migliori, G. Giordano, F.
6 Frusteri, Interaction effects between CuO-ZnO-ZrO₂ methanol phase and zeolite surface
7 affecting stability of hybrid systems during one-step CO₂ hydrogenation to DME, *Catal*
8 *Today*. 345 (2020) 175–182. <https://doi.org/10.1016/J.CATTOD.2019.08.014>.
- 9 [11] E. Catizzone, A. Aloise, M. Migliori, G. Giordano, Dimethyl ether synthesis via methanol
10 dehydration: Effect of zeolite structure, *Appl Catal A Gen*. 502 (2015) 215–220.
11 <https://doi.org/10.1016/J.APCATA.2015.06.017>.
- 12 [12] P. Lanzafame, G. Papanikolaou, S. Perathoner, G. Centi, M. Migliori, E. Catizzone, A. Aloise,
13 G. Giordano, Direct versus acetalization routes in the reaction network of catalytic HMF
14 etherification, *Catal Sci Technol*. 8 (2018) 1304–1313. <https://doi.org/10.1039/C7CY02339A>.
- 15 [13] J.R. Plaisier, L. Nodari, L. Gigli, E.P.R.S. Miguel, R. Bertocello, A. Lausi, The X-ray
16 diffraction beamline MCX at Elettra: a case study of non-destructive analysis on stained glass,
17 *Acta IMEKO*. 6 (2017) 71–75. https://doi.org/10.21014/ACTA_IMEKO.V6I3.464.
- 18 [14] L. Rebuffi, J.R. Plaisier, M. Abdellatif, A. Lausi, A.P. Scardi, MCX: a Synchrotron
19 Radiation Beamline for X-ray Diffraction Line Profile Analysis, *Z Anorg Allg Chem*. 640
20 (2014) 3100–3106. <https://doi.org/10.1002/ZAAC.201400163>.
- 21 [15] A.C. Larson, R.B. Von, D. Lance, GSAS GENERAL STRUCTURE ANALYSIS SYSTEM,
22 (n.d.).

- 1 [16] B.H. Toby, IUCr, EXPGUI, a graphical user interface for GSAS, *Urn:Issn:0021-8898*. 34
2 (2001) 210–213. <https://doi.org/10.1107/S0021889801002242>.
- 3 [17] D.H. Olson, G.T. Kokotailo, S.L. Lawton, W.M. Meier, Crystal structure and structure-related
4 properties of ZSM-5, *Journal of Physical Chemistry*. 85 (1981) 2238–2243.
5 https://doi.org/10.1021/J150615A020/SUPPL_FILE/J150615A020_SI_001.PDF.
- 6 [18] Y. Yokomori, S. Idaka, The structure of TPA-ZSM-5 with Si/Al=23, *Microporous and*
7 *Mesoporous Materials*. 28 (1999) 405–413. [https://doi.org/10.1016/S1387-1811\(98\)00311-4](https://doi.org/10.1016/S1387-1811(98)00311-4).
- 8 [19] K.J. Chao, J.C. Lin, Y. Wang, G.H. Lee, Single crystal structure refinement of TPA ZSM-5
9 zeolite, *Zeolites*. 6 (1986) 35–38. [https://doi.org/10.1016/0144-2449\(86\)90009-6](https://doi.org/10.1016/0144-2449(86)90009-6).
- 10 [20] H. Lerner, M. Draeger, J. Steffen, K.K. Unger, Synthesis and structure refinement of ZSM—
11 5 single crystals, *Zeolites*. 5 (1985) 131–134. [https://doi.org/10.1016/0144-2449\(85\)90019-3](https://doi.org/10.1016/0144-2449(85)90019-3).
- 12 [21] G.D. Price, J.J. Pluth, J. V. Smith, J.M. Bennett, R.L. Patton, Crystal Structure of
13 Tetrapropylammonium Fluoride Containing Precursor to Fluoride Silicalite, *J Am Chem Soc*.
14 104 (1982) 5971–5977.
15 https://doi.org/10.1021/JA00386A023/SUPPL_FILE/JA00386A023_SI_001.PDF.
- 16 [22] R.D. Shannon, IUCr, Revised effective ionic radii and systematic studies of interatomic
17 distances in halides and chalcogenides, *Urn:Issn:0567-7394*. 32 (1976) 751–767.
18 <https://doi.org/10.1107/S0567739476001551>.
- 19 [23] A. Lobato, H.H. Osman, M.A. Salvadó, M. Taravillo, V.G. Baonza, J.M. Recio, Chemical
20 pressure–chemical knowledge: squeezing bonds and lone pairs within the valence shell
21 electron pair repulsion model, *Physical Chemistry Chemical Physics*. 21 (2019) 12585–12596.
22 <https://doi.org/10.1039/C9CP00913B>.

- 1 [24] H.H. Osman, M.A. Salvadó, P. Pertierra, J. Engelkemier, D.C. Fredrickson, J.M. Recio,
2 Chemical Pressure Maps of Molecules and Materials: Merging the Visual and Physical in
3 Bonding Analysis, *J Chem Theory Comput.* 14 (2018) 104–114.
4 [https://doi.org/10.1021/ACS.JCTC.7B00943/ASSET/IMAGES/LARGE/CT-2017-](https://doi.org/10.1021/ACS.JCTC.7B00943/ASSET/IMAGES/LARGE/CT-2017-00943E_0011.JPEG)
5 [00943E_0011.JPEG](https://doi.org/10.1021/ACS.JCTC.7B00943/ASSET/IMAGES/LARGE/CT-2017-00943E_0011.JPEG).
- 6 [25] L.B. McCusker, D.H. Olson, C. Baerlocher, *Atlas of Zeolite Framework Types*, Atlas of
7 Zeolite Framework Types. (2007). <https://doi.org/10.1016/B978-0-444-53064-6.X5186-X>.
- 8 [26] P. Fejes, J.B. Nagy, J. Halász, A. Oszkó, Heat-treatment of isomorphously substituted ZSM-5
9 zeolites and its structural consequences: An X-ray diffraction, ²⁹Si MAS-NMR, XPS and FT-
10 IR spectroscopy study, *Appl Catal A Gen.* 175 (1998) 89–104. [https://doi.org/10.1016/S0926-](https://doi.org/10.1016/S0926-860X(98)00212-9)
11 [860X\(98\)00212-9](https://doi.org/10.1016/S0926-860X(98)00212-9).
- 12 [27] G. Cruciani, Zeolites upon heating: Factors governing their thermal stability and structural
13 changes, *Journal of Physics and Chemistry of Solids.* 67 (2006) 1973–1994.
14 <https://doi.org/10.1016/J.JPCS.2006.05.057>.
- 15 [28] M. Milanesio, G. Artioli, A.F. Gualtieri, L. Palin, C. Lamberti, Template Burning inside TS-1
16 and Fe-MFI Molecular Sieves: An in Situ XRPD Study, (2003).
17 <https://doi.org/10.1021/JA037229>.
- 18 [29] L. Leardini, A. Martucci, A. Alberti, G. Cruciani, Template burning effects on stability and
19 boron coordination in boron lewyne studied by in situ time resolved synchrotron powder
20 diffraction, *Microporous and Mesoporous Materials.* 167 (2013) 117–126.
21 <https://doi.org/10.1016/J.MICROMESO.2012.02.013>.
- 22 [30] A. Martucci, M. de L. Guzman-Castillo, F. Di Renzo, F. Fajula, A. Alberti, Reversible
23 channel deformation of zeolite omega during template degradation highlighted by in situ time-

- 1 resolved synchrotron powder diffraction, *Microporous and Mesoporous Materials*. 104 (2007)
2 257–268. <https://doi.org/10.1016/J.MICROMESO.2007.02.040>.
- 3 [31] S. Sen, R.R. Wusirika, R.E. Youngman, High temperature thermal expansion behavior of
4 H[Al]ZSM-5 zeolites: The role of Brønsted sites, *Microporous and Mesoporous Materials*. 87
5 (2006) 217–223. <https://doi.org/10.1016/J.MICROMESO.2005.08.010>.
- 6 [32] M. Ardit, A. Martucci, G. Cruciani, Monoclinic orthorhombic phase transition in ZSM 5
7 zeolite: Spontaneous strain variation and thermodynamic properties, *Journal of Physical*
8 *Chemistry C*. 119 (2015) 7351–7359.
9 https://doi.org/10.1021/ACS.JPCC.5B00900/ASSET/IMAGES/JP-2015-00900A_M015.GIF.
- 10 [33] D.S. Bhange, V. Ramaswamy, Negative thermal expansion in silicalite-1 and zirconium
11 silicalite-1 having MFI structure, *Mater Res Bull*. 41 (2006) 1392–1402.
12 <https://doi.org/10.1016/J.MATERRESBULL.2005.12.002>.

13

14



Click here to access/download
Supplementary Material
Supplementary Information.docx



Declaration of interests

The authors declare that they have no known competing financial interests or personal relationships that could have appeared to influence the work reported in this paper.

The authors declare the following financial interests/personal relationships which may be considered as potential competing interests: